THE JOURNAL OF PHYSICAL CHEMISTRY B

Article

pubs.acs.org/JPCB

Ferryl–Oxo Species Produced from Fenton's Reagent via a Two-Step Pathway: Minimum Free-Energy Path Analysis

Norifumi Yamamoto,[†,‡,§] Nobuaki Koga,*[,†,‡] and Masataka Nagaoka*[,†,‡]

[†]Graduate School of Information Science, Nagoya University, Furo-cho, Chikusa-ku, Nagoya 464-8601, Japan

[‡]CREST Project, Japan Science and Technology Agency, 4-1-8 Honcho, Kawaguchi, Saitama 332-0012, Japan

ABSTRACT: A mixture of ferrous ions and hydrogen peroxide, known as Fenton's reagent, is an effective oxidant and has been widely used in various industrial applications; however, there is still controversy about what the oxidizing agents are and how they are produced. In this study, we have determined minimum free-energy paths (MFEPs) from Fenton's reagent to possible oxidizing agents such as hydroxyl radicals and ferryl–oxo species by combining ab initio molecular dynamics simulations and an MFEP search method. Along the MFEPs, representative free-energy profiles of the Fenton reaction were elucidated. On the basis of the free-energy profiles, we revealed that the reaction producing ferryl–oxo species from Fenton's reagent is more energetically favorable than that yielding a free hydroxyl radical, by 24.4 kcal mol^{-1}, which indicates that the ferryl–oxo species is the primary oxidizing agent in reactions of Fenton's reagent. Moreover, we clarified that the ferryl–oxo species is favorably formed via a two-step reaction pathway, which reaches the product through a dihydroxyiron(IV) intermediate. The energetics charting the free-energy profiles provided valuable information for a comprehensive understanding of Fenton reactions. We concluded that a ferryl–oxo species produced from Fenton's reagent serves as the primary oxidizing agent in the Fenton reaction.

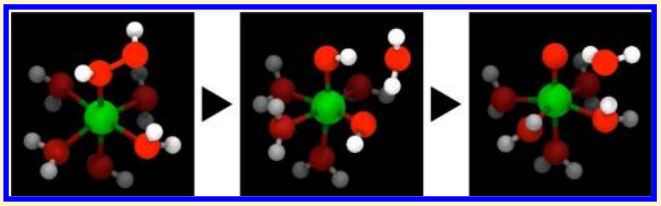

I. INTRODUCTION

Fenton's reagent is a mixture of ferrous ions and hydrogen peroxide,[1] and is known to be an effective oxidant in aqueous solutions.[2] Since both iron and hydrogen peroxide are environmentally safe substances, Fenton's reagent and its analogues are used as *green* oxidants in a broad range of industrial applications such as wastewater treatment[3] and groundwater remediation.[4] In the natural environment, the Fenton reaction occurs ubiquitously in sunlit natural waters[5] because ferrous ions are common constituents of seawater and alkaline freshwater,[6] and photochemical formation of hydrogen peroxide has been observed in waters exposed to sunlight.[7] The reactions of Fenton's reagent have also been cited as models for biological processes[8] such as metal-mediated oxidative damage.[9] More intriguingly, iron(II)–H_2O_2 precursors are involved in oxidation of substrates in enzymatic systems[10] such as cytochrome P450.[11] The chemistry of Fenton's reagent is therefore the subject of intense interest in both pure and applied chemistry; however, there remains considerable controversy regarding its reaction mechanism.[12−19] The key controversial issue concerns the oxidizing agents in the Fenton reaction.

The hydroxyl radical, HO$^{\bullet}$, which is generated by dissociation of hydrogen peroxide, catalyzed by ferrous ions, has generally been assumed to be the potent agent that oxidizes substrates in the Fenton reaction.[20] It is considered that a pentaaquairon(II)–H_2O_2 complex **1** serves as a precursor for the formation of a hydroxyl radical:[21]

$$[Fe^{II}(H_2O_2)(H_2O)_5]^{2+}\ (\mathbf{1}) \rightarrow [Fe^{III}(OH^-)(H_2O)_5]^{2+} + OH^{\bullet} \quad (1)$$

A high-valent ferryl–oxo species, $[Fe^{IV}(O^{2-})]^{2+}$ (**2**), has alternatively been proposed as the oxidizing agent in the Fenton reaction.[22] Despite numerous studies, there is ongoing controversy regarding identification of the oxidizing agents in the Fenton reaction because of the experimental difficulties of detecting such transient species.

Complementary to experiments, computational studies are helpful in elucidating the reaction mechanism of Fenton's reagent. Baerends and co-workers have investigated the reactions of Fenton's reagent using electronic structure calculations and ab initio molecular dynamics (MD) simulations.[23−30] They demonstrated that ferryl–oxo complex **2** is the most likely candidate as the active oxidizing agent, and that it could be produced in two different ways.[23−26] One follows a pathway that leads to **2** directly from **1**:

$$[Fe^{II}(H_2O_2)(H_2O)_5]^{2+}\ (\mathbf{1}) \rightarrow [Fe^{IV}(O^{2-})(H_2O)_5]^{2+}\ (\mathbf{2}) + H_2O \quad (2)$$

The other follows a pathway with two reaction steps, which yields **2** from **1** indirectly via a dihydroxyiron(IV) intermediate **3**:

$$[Fe^{II}(H_2O_2)(H_2O)_5]^{2+}\ (\mathbf{1}) \rightarrow [Fe^{IV}(OH^-)_2(H_2O)_4]^{2+}\ (\mathbf{3}) + H_2O \quad (3a)$$

$$[Fe^{IV}(OH^-)_2(H_2O)_4]^{2+}\ (\mathbf{3}) \rightarrow [Fe^{IV}(O^{2-})(H_2O)_5]^{2+}\ (\mathbf{2}) \quad (3b)$$

Received: October 9, 2012
Published: November 13, 2012

dx.doi.org/10.1021/jp310008z | J. Phys. Chem. B 2012, 116, 14178−14182

The energetics of reaction 3 was revealed in vacuo using electronic structure calculations.[23,25] The dynamics in the formation of ferryl−oxo species, depicted in eqs 2 and 3, has been successfully simulated in the presence of solvent water molecules using ab initio MD simulations.[24−26] The issue of energetics *in aqueous solutions*, however, which is indispensable for a comprehensive understanding of the Fenton reaction, remains uncertain.

In this study, we intend to address what the oxidizing agent is in the Fenton reaction, and how it is produced. For this purpose, we report free-energy profiles for the reactions of Fenton's reagent, depicted in eqs 1−3. A unique feature of this study is determination of the minimum free-energy paths (MFEPs) from Fenton's reagent to possible oxidizing species, not only hydroxyl radicals, but also ferryl−oxo complexes formed via two different reaction pathways; this enables us to properly understand the reactions of Fenton's reagent from a unified viewpoint. We have observed clear differences in the free-energy changes along the MFEPs for reactions 1−3 of Fenton's reagent.

II. COMPUTATIONAL METHODS

We determined the MFEPs for the reactions of Fenton's reagent to produce oxidizing agents, using the string method[31] combined with ab initio MD simulations.

The string method is the path-search method developed by Vanden-Eijnden and co-workers;[31] it defines the MFEP as a string of replicas. The essence of the method is to evolve the string according to the free-energy gradient,[32,33] so that it makes the string converge toward the MFEP in a reduced space of collective variables, with all the other degrees of freedom integrated out. This can be achieved by performing MD simulations for each replica with restraints imposed on selected collective variables. In our approach, six interatomic distances, Fe−O_α, O_α−O_β, O_α−H_α, O_β−H_α, O_β−H_γ, and O_γ−H_γ, shown in Chart 1, were selected as the collective variables. Each MFEP

Chart 1. Schematic Representation of Complex 1

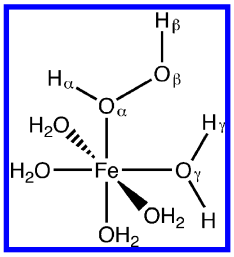

was defined by a string of 21 replicas connecting the reactant and product states. The reaction coordinate parameter $\sigma \in [0,1]$ was used to parametrize the MFEP. The ab initio MD simulations were performed with restraints for the reaction coordinates at the 21 points on the MFEP thus determined. From the resulting restrained MD simulations, the free-energy changes along the MFEP were computed as functions of σ.

The ab initio MD simulations were performed within the Car−Parrinello scheme.[34] The electronic structure of the valence electrons was described by density functional theory, using the Perdew−Burke−Ernzerhof functional,[35] expanded in plane waves with an energy cutoff of 25 Ry and a density cutoff of 150 Ry. The core electrons were represented by the Vanderbilt ultrasoft pseudopotentials.[36] The temperature was kept at 300 K using a Nosé−Hoover thermostat. In all the electronic structure calculations, the high-spin quintet state was considered, following previous calculations.[23−26] The MD time-step was 0.121 fs and the fictitious electronic mass for the electronic degrees of freedom was 500 au. The model consisted of one iron ion, one hydrogen peroxide molecule, and 31 water molecules in a periodic cubic box of side length 9.957 Å. All H−O bond distances in the water molecules, except for the pairs selected as collective variables, were constrained to be 0.9974 Å in order to strictly control chemical reactions in the system. For MFEP searches, the string of replicas was evolved over 300 times, based on the string method;[31] MD simulations were performed for 120.9 ps each time, with restraining selected interatomic distances using a harmonic potential with a force constant of 1000 kcal mol^{-1} $Å^{-2}$. After the MFEP searches, MD simulations with 30 000 steps were performed at the 21 points on the MFEP, with restraints for the reaction coordinates. From the resulting restrained MD simulations, the free-energy change along the MFEP was computed using an umbrella integration.[37] All the ab initio MD simulations were performed using the CPMD code.[38]

Previous ab initio MD simulations have shown that since the pentaaquairon(II)−H_2O_2 complex **1** is not a stable intermediate in aqueous solution, the O−O bond in the hydrogen peroxide ligand cleaves immediately.[24−26] In the present calculations of the reactant state, the O_α−O_β distance was therefore restrained to be 1.5 Å, which corresponds to the optimal bond distance of hydrogen peroxide in aqueous solution, in order to simulate its complex with pentaaquairon(II), **1**.

III. RESULTS

Reaction 1 yields a hydroxyl radical from **1** via O−O bond cleavage of H_2O_2. The free-energy profile for this reaction is shown in Figure 1, together with the change in collective

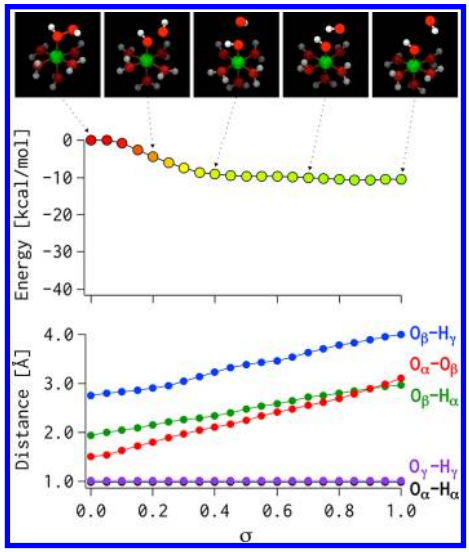

Figure 1. Free-energy profile and interatomic distances selected as collective variables along the MFEP of reaction 1, which yields an $HO^\bullet$ radical from **1**. Snapshots show changes in molecular structures along the MFEP.

variables along the MFEP. At the initial reactant state of $\sigma = 0$, most of the collective variables were free to evolve along the steepest descent, according to the free-energy gradient, except for O_α−O_β with a restrained distance. At the final product state of $\sigma = 1$, all the collective variables were free to evolve, and then

dx.doi.org/10.1021/jp310008z | J. Phys. Chem. B 2012, 116, 14178−14182

the O_α–O_β distance reached 3 Å, and the resulting $H_\beta O_\beta^\bullet$ radical was included in the second hydration shell around the $[Fe^{III}(OH^-)(H_2O)_5]^{2+}$ complex. As shown in Figure 1, the free-energy change along the MFEP is downhill by 10.5 kcal mol^{-1}, with no overall energy barrier. The free-energy change nearly reaches its final plateau value at σ = 0.4, where the O_α–O_β distance exceeds 2 Å. We therefore assume the criterion that an $H_\beta O_\beta^\bullet$ radical forms at the O_α–O_β distance of 2 Å as a consequence of bond cleavage,[26] and this will be used in the following discussions. The O–O bond cleavage in this reaction is an exergonic process and thus may occur spontaneously after H_2O_2 coordinates to a ferrous ion. As a matter of fact, the ab initio MD simulations illustrated that, starting from **1** in aqueous solution, the O–O bond of H_2O_2 cleaves immediately.[24−26] Without an iron catalyst, the homolytic O–O bond dissociation of H_2O_2 costs about 50 kcal mol^{-1}.[39] Moreover, the catalytic effect of ferrous iron in the O–O bond breaking of H_2O_2 has already been rationalized by electronic structure calculations, in which the iron-catalyzed reaction was considered to have a much smaller dissociation enthalpy of 27 kcal mol^{-1}, even in vacuo, but to be endothermic.[23] These results indicate that the spontaneous O–O cleavage in aqueous solution proceeds primarily as a result of solvation effects, which stabilize an Fe^{III}–$OH^-/HO^\bullet$ pair more than they stabilize the Fe^{II}–H_2O_2 state.

Reaction 2 gives ferryl–oxo species **2** from **1** immediately after formation of a hydroxyl radical. The free-energy profile and the changes in collective variables for this reaction are summarized in Figure 2. In the initial stage of the reaction, until

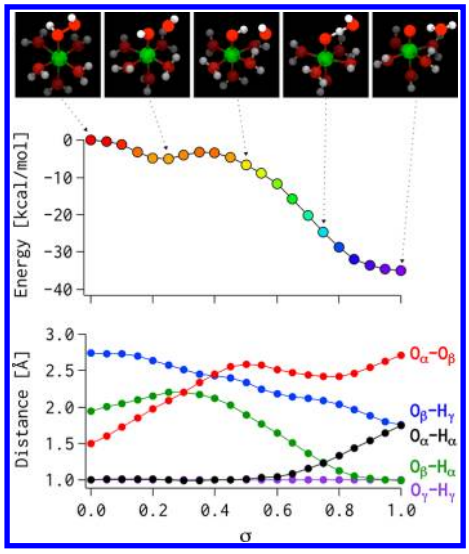

Figure 2. Free-energy profile and interatomic distances selected as collective variables along the MFEP of reaction 2, which yields ferryl–oxo complex **2** from **1**. Snapshots show changes in molecular structures along the MFEP.

σ = 0.25, the free-energy curve is downhill, where the O_α–O_β distance exceeds 2 Å and an $H_\beta O_\beta^\bullet$ radical forms, as observed in reaction 1. This initial step is exergonic by 5.0 kcal mol^{-1}. In the intermediate stage, until σ = 0.5, following O–O cleavage, a characteristic maximum in the free-energy change appears at around σ = 0.35, where the free-energy value rises to −3.3 kcal mol^{-1}, and thus the activation free-energy is 1.7 kcal mol^{-1}. In the region from σ = 0.25 to 0.5, which includes the maximal point, the O_α–O_β distance increases, whereas the O_β–H_α distance decreases. The O_α–H_α–O_β bond angles calculated using the bond distances are 70°, 86°, and 124° at σ = 0.25, 0.35, and 0.5, respectively, along the MFEP. The results clearly indicate that the resulting $H_\beta O_\beta^\bullet$ radical moves around the $O_\alpha H_\alpha$ ligand with an energy barrier of 1.7 kcal mol^{-1}, so the O_β atom accepts a hydrogen bond from the $O_\alpha H_\alpha$ ligand. In the last stage, immediately after formation of the hydrogen bond, the $H_\beta O_\beta^\bullet$ radical abstracts the H_α atom from the $O_\alpha H_\alpha$ ligand to yield **2** and a newly formed $H_\beta O_\beta H_\alpha$ molecule. In this stage, the shortening of the O_α–O_β distance is found to facilitate H_α atom transfer. A considerable energy of 28.2 kcal mol^{-1} is released in this final step from σ = 0.5 to 1, and the total free-energy change reaches −34.9 kcal mol^{-1}. The total free-energy of this reaction shows good agreement with previous electronic structure calculations, where the corresponding value was estimated to be −34 kcal mol^{-1}.[25]

Reaction 3 leads to the formation of ferryl–oxo species **2** by a different route from reaction 2, through formation of the dihydroxyiron(IV) complex **3**, as depicted in eq 3a. The results for this reaction are shown in Figure 3. The O_α–O_β distance

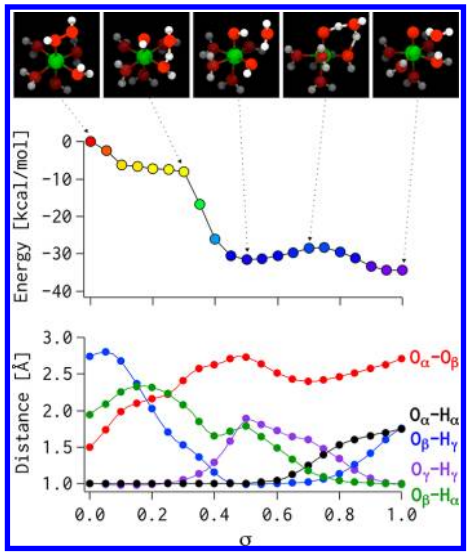

Figure 3. Free-energy profile and interatomic distances selected as collective variables along the MFEP of reaction 3, which yields ferryl–oxo complex **2** from **1** through the dihydroxyiron(IV) complex **3**. Snapshots show changes in molecular structures along the MFEP.

reaches the cleavage length of 2 Å at σ = 0.1, where the free-energy falls to −6.3 kcal mol^{-1}. A gentle free-energy slope follows after this O–O bond cleavage. In this step, ranging from σ = 0.1 to 0.3, as the O_α–O_β distance increases gradually, the O_β–H_γ distance decreases rapidly. This indicates that the $H_\beta O_\beta^\bullet$ radical approaches one of the water ligands, $HO_\gamma H_\gamma$, and then forms a hydrogen bond, accompanied by a free-energy change of −1.7 kcal mol^{-1}, without an energy barrier. The formation of the hydrogen bond can therefore occur spontaneously, which is a characteristic difference from the corresponding process in reaction 2. This result indicates that the $H_\beta O_\beta^\bullet$ radical, formed by O–O bond cleavage of $H_\beta O_\beta O_\alpha H_\alpha$ in **1**, prefers to move toward the $HO_\gamma H_\gamma$ ligand to form a hydrogen bond rather than rebounding with the $H_\alpha O_\alpha$ moiety. After formation of the hydrogen bond, the H_γ atom transfers from the $HO_\gamma H_\gamma$ ligand to the $H_\beta O_\beta^\bullet$ radical, leading to **3** at σ = 0.5, with a relative free-energy of −31.5 kcal mol^{-1}. The total change in the free-energy of the reaction is smaller than that of reaction 2 by 3.4 kcal mol^{-1}, which indicates that

dx.doi.org/10.1021/jp310008z | J. Phys. Chem. B 2012, 116, 14178−14182

the formation of ferryl−oxo complex **2** might be thermodynamically more favorable than formation of the dihydroxyiron(IV) complex **3**.

Complex **2** would therefore rearrange to **3**, as depicted in eq 3b. The free-energy profile of this reaction is also shown in Figure 3. In **3**, the $H_\beta O_\beta H_\gamma$ molecule, which is one of the products of reaction 3a, bridges two HO^- ligands through hydrogen bonds, where the $H_\alpha O_\alpha$ ligand serves as a proton donor and the HO_γ ligand serves as a proton acceptor. Starting from this hydrogen-bonded complex between $[Fe^{IV}(OH^-)_2(H_2O)_4]^{2+}$ and H_2O, proton transfers occur stepwise; the first proton transfer from the $H_\alpha O_\alpha$ ligand to the $H_\beta O_\beta H_\gamma$ molecule leads to a transition state with an $[H_\alpha O_\beta(H_\beta)H_\gamma]^+$ hydronium ion moiety at $\sigma = 0.7$, and then the second proton transfer occurs from this hydronium ion to the HO_γ ligand. This reaction, yielding **2** via double proton-transfer from **3**, is exergonic by 3.0 kcal mol^{-1}, with an energy barrier of 3.1 kcal mol^{-1}. Since the total free-energy does not depend on the reaction pathway, the value obtained directly from reaction 2 gives good agreement with that obtained from the two-step route. Furthermore, the height of the energy barrier is in agreement with the result of the corresponding electronic structure calculation, where the value was estimated to be 3.5 kcal mol^{-1}.[23]

IV. DISCUSSION

The purpose of this study was to clarify what the oxidizing agent in the Fenton reaction is, and how it is produced. For this purpose, we determined the MFEPs for the reactions from Fenton's reagent to possible oxidizing agents, depicted in eqs 1−3. From the results, we revealed typical differences in the free-energy profiles along the MFEPs for reactions 1−3, which provide a good basis for discussing the controversial problems regarding the reaction mechanism of Fenton's reagent.

As mentioned in the introduction, both hydroxyl radical and ferryl−oxo species are assumed to be potent oxidizing agents, and there is ongoing controversy over which is the active oxidizing agent in the Fenton reaction. As is obvious from the free-energy profiles, the total free-energy change for reactions 2 and 3 is much smaller than that for reaction 1, by 24.4 kcal mol^{-1}, which indicates that the reactions producing ferryl−oxo complex **2** are more thermodynamically favorable than the reaction yielding a free hydroxyl radical. Most previous studies have suggested that the ferryl−oxo species might be the oxidizing agent in the Fenton reaction;[16,22−30,40,41] however, no comprehensive understanding has been achieved. The free-energy profiles we obtained in this study give a decisive piece of evidence to support the suggestion that the ferryl−oxo species is the primary oxidizing agent produced in the reactions of Fenton's reagent.

The ferryl−oxo complex **2** could be produced from **1** in two different ways, as already demonstrated in previous studies.[23−26] One of these is the one-step pathway depicted in eq 2. The other is the two-step pathway, which yields **2** indirectly via **3**, depicted in eqs 3a and 3b. Our results demonstrate that these reactions start with spontaneous O−O bond cleavage of H_2O_2 in **1**, yielding $HO^\bullet$ and $[Fe^{III}(OH^-)(H_2O)_5]^{2+}$. As is evident from the free-energy profiles, the resulting $HO^\bullet$ fragment prefers the route involving approaching an adjacent H_2O ligand, i.e., reaction 3, to the route involving rebounding with an OH^- ligand, reaction 2. If the reaction of Fenton's reagent takes the former route, the $HO^\bullet$ radical interacts with the H_2O ligand without an energy barrier, as shown in Figure 3. In contrast, as shown in Figure 2, the latter route needs activation energy. It can therefore be deduced that the OH^- moiety in the $[Fe^{III}(OH^-)(H_2O)_5]^{2+}$ intermediate tends to form strong hydrogen bonds with the solvent water molecules instead of interacting with $HO^\bullet$, since an extra energy of 1.7 kcal mol^{-1} is required in reaction 2 to form the transient complex $[Fe^{III}(OH^-\cdots HO^\bullet)(H_2O)_5]^{2+}$. This fact might determine how the ferryl−oxo complex is produced in the reactions of Fenton's reagent. In previous studies, formation of the ferryl−oxo species has been successfully simulated using ab initio MD simulations;[24−26] however, the question of why the two-step pathway is preferred in the reaction has remained unclear. A promising clue to answering this question was found in the free-energy profiles; this indicates that the formation of ferryl−oxo complex **2** follows the two-step pathway from **1** via the intermediate **3**, avoiding the energy barrier in the one-step pathway.

V. CONCLUSIONS

We have investigated the free-energy profiles along the MFEPs from Fenton's reagent to oxidizing agents. The results show that after coordination of hydrogen peroxide to a ferrous ion in aqueous solution, yielding a pentaaquairon(II)−H_2O_2 complex, $[Fe^{II}(H_2O_2)(H_2O)_5]^{2+}$ (**1**), O−O bond cleavage of hydrogen peroxide can occur immediately. After O−O bond cleavage of H_2O_2, the exergonicity for the reaction producing a ferryl−oxo complex, $[Fe^{IV}(O^{2-})(H_2O)_5]^{2+}$ (**2**), is much larger than that for the reaction yielding a free $HO^\bullet$ radical. The ferryl−oxo complex **2** can be produced by two different pathways: the one-step pathway, forming **2** directly from **1**, and the two-step pathway, forming **2** indirectly from **1** via a dihydroxyiron(IV) complex, $[Fe^{IV}(OH^-)_2(H_2O)_4]^{2+}$ (**3**). On the basis of the free-energy profiles, we revealed that the two-step pathway is thermodynamically favored in the reaction, avoiding the energy barrier in the one-step pathway. These results lead to the conclusion that the primary oxidizing agent in the reactions of Fenton's reagent is the ferryl−oxo species **2**, which is formed from the pentaaquairon(II)−H_2O_2 complex **1** through a two-step pathway via the dihydroxyiron(IV) intermediate **3**.

The MFEP and the free-energy change along it are often the most informative quantities regarding the mechanism of a chemical reaction.[42] The energetics charting the MFEPs for the reactions of Fenton's reagent therefore provides not only valuable information for a comprehensive understanding of the Fenton reaction but also insights into a general understanding of iron-mediated catalytic reactions in solution.

AUTHOR INFORMATION

Corresponding Author

*E-mail: koga@is.nagoya-u.ac.jp (N.K.); mnagaoka@is.nagoya-u.ac.jp (M.N.).

Present Address

[§]Department of Life and Environmental Sciences, Faculty of Engineering, Chiba Institute of Technology, 2-17-1 Tsudanuma, Narashino, Chiba 275−0016, Japan

Notes

The authors declare no competing financial interest.

ACKNOWLEDGMENTS

This work was supported by the Core Research for Evolutional Science and Technology (CREST) "High Performance Computing for Multiscale and Multiphysics Phenomena" from the Japan Science and Technology Agency. N.Y. also thanks the Ministry of Education, Culture, Sports, Science and Technology in Japan for

support through Grants-in-Aid for Scientific Research and for Young Scientists (B) (23770175).

REFERENCES

(1) Fenton, H. J. H. *J. Chem. Soc. Trans.* **1894**, *65*, 899−910.
(2) Wardman, P.; Candeias, L. P. *Radiat. Res.* **1996**, *145*, 523−531.
(3) Bautista, P.; Mohedano, A. F.; Casas, J. A.; Zazo, J. A.; Rodriguez, J. J. *J. Chem. Tech. Biotechnol.* **2008**, *83*, 1323−1338.
(4) Watts, R. J.; Teel, A. L. *J. Environ. Eng.* **2005**, *131*, 612−622.
(5) Southworth, B. A.; Voelker, B. M. *Environ. Sci. Technol.* **2003**, *37*, 1130−1136.
(6) Hem, J. D. *U.S.G.S. Water-Supply Paper* **1985**, *2254*, 76−84.
(7) Cooper, W. J.; Zika, R. G. *Science* **1983**, *220*, 711−712.
(8) Prousek, J. *Pure Appl. Chem.* **2007**, *79*, 2325−2338.
(9) Jomova, K.; Valko, M. *Toxicology* **2011**, *283*, 65−87.
(10) Vlasits, J.; Jakopitsch, C.; Bernroitner, M.; Zamocky, M.; Furtmüller, P. G.; Obinger, C. *Arch. Biochem. Biophys.* **2010**, *500*, 74−81.
(11) Meunier, B.; de Visser, S. P.; Shaik, S. *Chem. Rev.* **2004**, *104*, 3947−3980.
(12) Rachmilovich-Calis, S.; Masarwa, A.; Meyerstein, N.; Meyerstein, D.; van Eldik, R. *Chem.—Eur. J.* **2009**, *15*, 8303−8309.
(13) Barbusiński, K. *Ecol. Chem. Eng.* **2009**, *16*, 347−358.
(14) Kremer, M. L. *J. Inorg. Biochem.* **2000**, *78*, 255−257.
(15) Goldstein, S.; Meyerstein, D. *Acc. Chem. Res.* **1999**, *32*, 547−550.
(16) Kremer, M. L. *Phys. Chem. Chem. Phys.* **1999**, *1*, 3595−3605.
(17) MacFaul, P. A.; Wayner, D. D. M.; Ingold, K. U. *Acc. Chem. Res.* **1998**, *31*, 159−162.
(18) Walling, C. *Acc. Chem. Res.* **1998**, *31*, 155−157.
(19) Sawyer, D. T.; Sobkowiak, A.; Matsushita, T. *Acc. Chem. Res.* **1996**, *29*, 409−416.
(20) Haber, F.; Weiss, J. *Proc. R. Soc. London, A* **1934**, 332−351.
(21) Goldstein, S.; Meyerstein, D.; Czapski, G. *Free Radical Biol. Med.* **1993**, *15*, 435−445.
(22) Bray, W. C.; Gorin, M. H. *J. Am. Chem. Soc.* **1932**, *54*, 2124−2125.
(23) Buda, F.; Ensing, B.; Gribnau, M. C. M.; Baerends, E. J. *Chem.—Eur. J.* **2001**, *7*, 2775−2783.
(24) Ensing, B.; Buda, F.; Blöchl, P.; Baerends, E. J. *Angew. Chem., Int. Ed.* **2001**, *40*, 2893−2895.
(25) Ensing, B.; Buda, F.; Blöchl, P. E.; Baerends, E. J. *Phys. Chem. Chem. Phys.* **2002**, *4*, 3619−3627.
(26) Ensing, B.; Baerends, E. J. *J. Phys. Chem. A* **2002**, *106*, 7902−7910.
(27) Ensing, B.; Buda, F.; Gribnau, M. C. M.; Baerends, E. J. *J. Am. Chem. Soc.* **2004**, *126*, 4355−4365.
(28) Louwerse, M. J.; Baerends, E. J. *Phys. Chem. Chem. Phys.* **2007**, *9*, 156−166.
(29) Louwerse, M. J.; Vassilev, P.; Baerends, E. J. *J. Phys. Chem. A* **2008**, *112*, 1000−1012.
(30) Michel, C.; Baerends, E. J. *Inorg. Chem.* **2009**, *48*, 3628−3638.
(31) Maragliano, L.; Fischer, A.; Vanden-Eijnden, E.; Ciccotti, G. *J. Chem. Phys.* **2006**, *125*, 024106−1−024106−15.
(32) Nagaoka, M.; Okuyama-Yoshida, N.; Yamabe, T. *J. Phys. Chem. A* **1998**, *102*, 8202−8208.
(33) Okuyama-Yoshida, N.; Nagaoka, M.; Yamabe, T. *Int. J. Quantum Chem.* **1998**, *70*, 95−103.
(34) Car, R.; Parrinello, M. *Phys. Rev. Lett.* **1985**, *55*, 2471−2474.
(35) Perdew, J. P.; Burke, K.; Ernzerhof, M. *Phys. Rev. Lett.* **1996**, *77*, 3865−3868.
(36) Vanderbilt, D. *Phys. Rev. B* **1990**, *41*, 7892−7895.
(37) Kästner, J.; Thiel, W. *J. Chem. Phys.* **2005**, *123*, 144104−1−144104−5.
(38) *CPMD*, version 3.15.1; IBM Corporation and MPI für Festkörperforschung: Stuttgart, Germany, 1997−2011.
(39) Bach, R. D.; Ayala, P. Y.; Schlegel, H. B. *J. Am. Chem. Soc.* **1996**, *118*, 12758−12765.
(40) Groves, J. T. *J. Inorg. Biochem.* **2006**, *100*, 434−447.
(41) Pestovsky, O.; Stoian, S.; Bominaar, E. L.; Shan, X.; Münck, E.; Que, L., Jr.; Bakac, A. *Angew. Chem., Int. Ed.* **2005**, *44*, 6871−6874.
(42) Hu, H.; Yang, W. *Annu. Rev. Phys. Chem.* **2008**, *59*, 573−601.